Contact Analysis Between a Moving Solid and the Boundary of its Swept Volume*

Hüseyin Erdim and Horea T. Ilieş†
Computational Design Laboratory
University of Connecticut‡
Email: *herdim,ilies*@engr.uconn.edu

Abstract

The modeling of many practical problems in design and manufacturing involving moving objects relies on sweeps and their boundaries, which are mathematically described by the envelopes to the family of shapes generated by the moving object. In many problems, such as the design and analysis of higher pairs or tool path planning, contact changes between the moving object and the boundary of its swept volume become critical because they often translate into functional changes of the system under consideration. However, the difficulty of this task quickly escalates beyond the reach of existing approaches as the complexity of the shape and motion increases.

We recently proposed a sweep boundary evaluator for general sweeps in conjunction with efficient point sampling and surface reconstruction algorithms that relies on our novel point membership classification (PMC) test for general solid sweeps. In this paper we describe a new approach that automates the prediction of changes in the state of contact between a shape of arbitrary complexity moving according to an affine motion, and the boundary of its swept set. We show that we can predict when and where such contact changes occur with only minimal additional computational cost by exploiting the data output by our sweep boundary evaluator. We discuss the problem and the associated computational issues in a 2D framework, and we conclude by discussing the extension of our approach to 3D moving objects.

*Proceedings of ASME IDETC08 Design Automation Conference. New York, August 2008

†Corresponding author.

‡Department of Mechanical Engineering, Storrs, CT 06269-3139

1 Introduction

A mechanism can be defined as a combination of connected bodies that move together to perform a particular (mechanical) function. A kinematic pair consists of two objects for which the relative motion between the objects depends on the position, shape and continuous contact between the objects. Depending on the type of contact between the objects, kinematic pairs are classified into lower pairs (of exactly six types see [1]) and higher pairs. The lower pairs are designed such that the coupling between the two objects that comprise the pair occurs over a surface. Theoretically, all other kinematic pairs are higher pairs, which represents a common and useful abstraction in the design and analysis of many problems involving contact between moving objects [2]. The geometry and motion of a higher pair are considerably more complex than those of a lower pair, which is why the design and analysis of higher pairs are, in general, non-trivial tasks.

Many practical design and manufacturing problems involving moving mechanical parts can be modeled by using sweeps, such as the cam-follower, gear or guiding mechanisms. In these cases, the generator, which can be one of the objects of the pair, is swept and the complement of the sweep is used to define the other object that completes the higher pair. The boundaries of these sweeps are mathematically described by the envelopes to the family of shapes generated by the moving object, which are tangent to every member of the family during the motion [3, 4, 5]. One of the critical analyses of higher pairs is the study of changes in the state of contact between the objects that comprise the higher pair because such changes often translate into functional changes of the system under consideration. In the mathematical realm, this translates into the study of critical points (or singularities) of the functions defining the envelopes [6].

Notably, the existence of these singularities in the envelopes of a moving object are an indication that loss of contact may occur between the moving object and the boundary of its swept set. This is important because the contact boundaries of any object that may move in contact with the moving shape during a prescribed motion must be a subset of the boundary of set swept by the moving object [7]. The traditional methods addressing the loss of contact in higher pairs, also known as *undercutting*, restrict the shape or motion of the moving object and thus the geometry of the kinematic pair, and often require difficult numerical computations, which, in turn, limits their applicability [8, 9, 10, 11, 12, 13, 14, 15, 16, 17, 18]. Importantly, undercutting conditions for some classes of mechanisms, such as wormgears, do not seem to be known today.

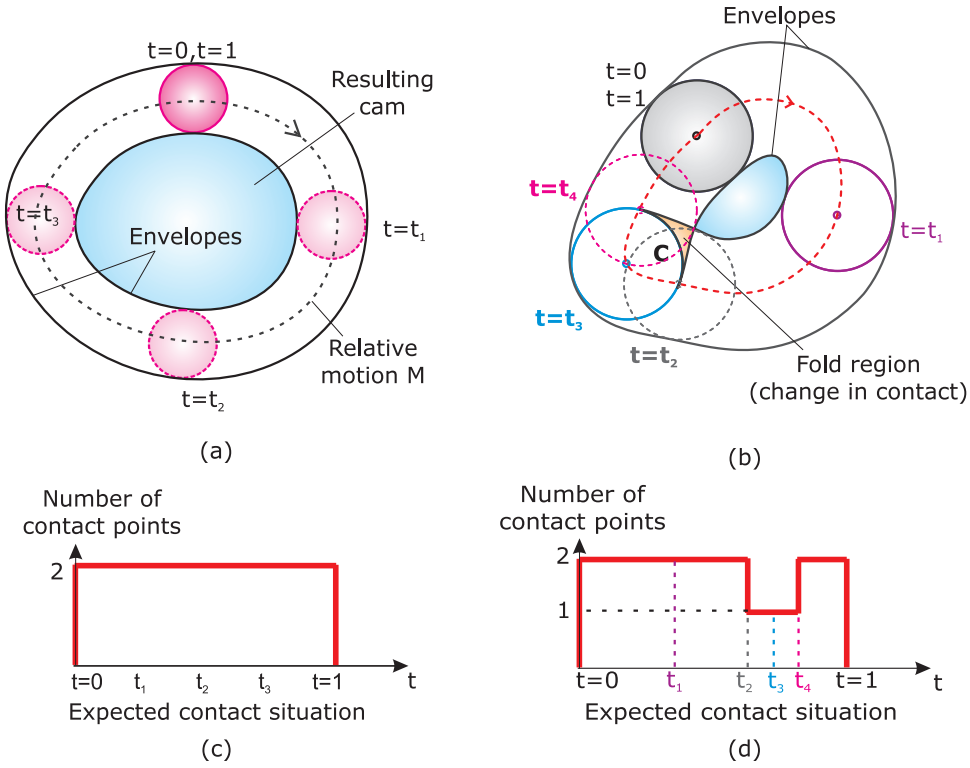

Figure 1: Typical relative motion of a cylindrical cam-follower mechanism: no change in the state of contact occurs in (a) and this is reflected in a constant number of contact points in (c); contact changes and undercutting occur in (b) as illustrated in the graph shown in (d).

Consider the simple cam-roller follower mechanism illustrated in Figure 1(a). Regardless of the size of the follower, it is easy to construct motions for which loss of contact occurs as shown in Figure 1(b). When undercutting is not present, there are two points of contact between the circular follower and the boundary envelopes as seen in Figures 1(a) and (c). The occurrence of undercutting induces a change in the number of contact points, and the evolution of this change for the case shown in Figure 1(b) is illustrated in Figure 1(d).

The closed form solutions for the existence of undercutting published in the literature can indeed be applied to simple cases such as the cam-follower

mechanism shown in Figure 1. However, such solutions exist only for a couple of simple cases among the many that can be encountered in practice. In more complex situations, engineers must still rely on their intuition and experience to perform the contact analysis. Alternatively, configuration spaces have been proposed both as a design tool [19] or as an analysis tool [20] for problems involving higher pairs. The study of contacts in configuration spaces is very appealing from a conceptual point of view because all contact configurations are represented as geometric entities in these spaces (i.,e., points, curves or surfaces). However, these (inevitably) higher dimensional configuration spaces are constructed today only for planar motions and objects that can be abstracted by piecewise linear geometries, which limits their practical use.

We recently introduced a point membership classification (PMC) test for general solid sweeping [21, 22], which classifies *all* points of space in which the object moves into "in", "on" and "out" points relative to the set swept by the moving object. Our classification includes points that are in the undercutting region, called fold points and fold regions - see Figure 1(b), or points that are on both boundary and internal envelopes[1]. Moreover, we have shown that our PMC test can be the basis of a stand-alone boundary evaluator for general solid sweeping in conjunction with space sampling algorithms [23]. This PMC test does not only provide complete geometric information about the swept set, but can also return the parameters of the motion that correspond to the instance when the boundary of the original object passes through a given point of the sweep [6]. We briefly revisit this issue in Section 2.

The central theme of this paper is that generating the point cloud corresponding to the sweep boundary points based on our PMC test provides the information needed to estimate the number of points of contact between the moving object and the boundary of the sweep at any configuration during the motion. Thus, changes in the state of contact between a moving object and its envelopes will be revealed by changes in the computed number of contact points. More importantly, these contact changes can be detected with practically negligible additional computational cost for solids of arbitrary complexity moving according to general affine motions. To the best of our knowledge, this paper presents the first known approach that can predict when and where contact changes occur within a higher pair of arbitrary complexity.

[1]The *internal* envelopes are interior to the set swept by the moving object. For details, see [21, 22].

The paper is organized as follows. Section 2 introduces our approach for estimating the number of contact points for 2-dimensional solids in planar motion. We illustrate the capability of this approach in section 3 by examining contact changes in three common planar higher pairs. Our last section summarizes the main features and limitations of our approach and discusses its extension to 3D.

2 Detecting Changes in the State of Contact

Contact analysis involves parts that move relative to each other. In mechanical design we focus on cases when the moving generator object S is a d-dimensional solid moving in d-dimensional Euclidean space $\mathbb{E}^d$, and $d = 2, 3$. In this paper we assume that $d = 2$ and that motion M is a one parameter family of transformations $M(t)$, where parameter $t \in [0, 1]$ belongs to a normalized unit interval. Observe that any interval $[a, b]$ can be normalized to a unit interval $[0, 1]$ without placing any additional restrictions on the problem at hand.

In an absolute coordinate system, each point y of an object S that moves according to M describes a trajectory $T_y = \{y^q \mid q \in M\}$. However, when observed from a moving coordinate system rigidly attached to the moving set S, the same point y will appear to describe a different trajectory denoted by $\hat{T}_y$. This *inverted trajectory* curve $\hat{T}_y$ can be computed not only for points of S, but also for any other point $x \in \mathbb{E}^d$ of the space as

$$\hat{T}_x = \{x^q \mid q \in \hat{M}\},$$

where $\hat{M}$ is the *inverted motion* defined as the inverse of $M(t)$ for every value of t [5]. It is not difficult to show that the inverted trajectory $\hat{T}_x$ of a point x contains *all* points of space $\mathbb{E}^d$ that pass through the given point x when moved according to motion M [24]. Furthermore, both T and $\hat{T}$ can be (re)parameterized in a manner consistent with the parametrization of motion $M(t)$.

2.1 Contact Analysis via Sweep Boundary Evaluation

Our PMC test described in [22] is defined in terms of inverted trajectory tests against the original geometric representation of the generator object S. More precisely, by intersecting the inverted trajectory of any point x of the space with the generator S in its initial configuration, one can classify point x as being "in", "on" or "out" relative to the set swept by S. In fact our

PMC test induces a finer decomposition of the space because the "in" points are themselves classified into regular, fold and fold boundary points – see [21] for details. Importantly, this test can be implemented in any geometric representation that supports curve-solid intersections.

If motion M and inverted trajectories $\hat{T}_x$ are consistently parameterized, then this intersection test outputs not only the correct classification of point x relative to the swept set, but also the parameters t of motion M when boundary points of S pass through x during M. Importantly, these boundary points (if they exist) are the only boundary points of S that would pass through the given x during M [24].

The ability to perform the PMC implies that one could sample the space in which the object moves and perform the sweep boundary evaluation. One approach is described in [23] where we used an octree decomposition of the space as a sampling strategy, but other approaches such as marching cubes [25] or Monte Carlo based sampling could be also employed. Through post-processing of these sweep boundary points and corresponding parameter values, we can actually compute the number of (sampled) contact points between S and its boundary envelopes that fall within specific parameter intervals. Note that these computations require only postprocessing of existing data comprised of points on the boundary of the sweep and their associated parameter values. Thus, as the motion parameter increases monotonically, a sudden change in the number of contact points would indicate a change in the state of contact between the moving object S and its envelopes that are on the boundary of the set $\texttt{sweep}(S, M)$. For the example shown in Figure 1(b), the follower initially has two contact points with the boundary of its swept set, but this state of contact changes as the prescribed motion progresses.

Parametric Discretization

A straightforward algorithm to count the number of contact points can be developed by discretizing the parameter interval into smaller subintervals of, say, equal lengths followed by counting the number of points that fall within every particular interval. In other words, one can employ a parametric discretization to count the number of contact points. By examining the number of points that fall within two such successive intervals, one can detect large changes in the number of contact points between adjacent intervals. A pseudo code of this algorithm is shown in Algorithm 1.

Vector $\mathbf{x}$ contains the list of boundary points of $\texttt{sweep}(S, M)$ output by the boundary evaluator. For each such point x_i, the boundary evaluator

input : (a) vector of points $\mathbf{x}$ together with an array of vectors of parameter values such that each x_i has a vector of parameters $\mathbf{t}_i = [t_{i0}, t_{i1}, ..., t_{ik}]$ for $k \in \mathbb{N}$;
(b) length Δ_t of the parameter subinterval;

output: parameter ranges of motion $M(t)$ where the state of contact between S and its boundary envelopes is changing;

1 Discretize the parameter interval $[0, 1]$ based on the prescribed subinterval Δ_t;
2 Sort all points x_i of $\mathbf{x}$ based on the values of $\mathbf{t}_i$ of x_i. Point x_i will appear in the sorted list for every parameter value in its vector of parameters $\mathbf{t}_i$;
3 Count the number of points in each parameter interval, and store the number of points in the i^{th} interval as n_i;
4 Determine "large" changes in the number of points between adjacent parameter intervals, i.e., between n_i and n_{i+1};
5 Output the intervals that have a "significantly different" number of points relative to the adjacent intervals;

Algorithm 1: An outline of the algorithm for detecting contact changes between a moving solid and the boundary of its swept set based on parametric discretization.

returns a list of parameter values where boundary points of S will pass through x_i. Observe that what is considered in step 5 of the algorithm to be a "significantly different" change in the number of contact points will strongly depend on the dimension of the space and on the sampling algorithm being used.

To illustrate the output of this algorithm, consider a 2-dimensional disk moving according to a planar rigid body motion such that the center of the disk moves along a semicircle or an elliptical trajectory as shown in Figure 2. Algorithm 1 outputs the data shown in Figure 2(c) for the circular motion during which the disk has exactly two contact points with its envelopes throughout the motion. During the elliptical motion, the state of contact between the disk and its boundary envelopes is changing, and the output of Algorithm 1 for that motion is shown in Figure 2(d). One can see that even though the parameter intervals do not contain a constant number of points, due in this case to the non-uniformity of the sampling[2], there are no sudden

[2]The octree cells are aligned with the coordinate axes in this example. Therefore the

(and large) jumps in the number of points between successive intervals in Figure 2(c). On the other hand, large jumps in the number of points are apparent in Figure 2(d) that corresponds to the elliptical trajectory.

In some cases, a correct interpretation of these results may be difficult because the changes in the computed number of contact points may not be sufficiently large. In a few words, this issue occurs because we are sampling in the Euclidean space, but we are counting points in the parameter space, and the two spaces do not share the same distance metric.

Geometric discretization

A better alternative is to perform first a uniform discretization of the point cloud containing points of the envelopes into elementary boundary units, and then translate these geometric units of equal size into (non-uniform) parametric intervals in the parameter space. Since our sampling uses octrees, and since all our partial octree cells that capture boundary points have the same size, we use a "Manhattan" distance metric to measure these elementary boundary units. This is illustrated in Figure 3(a). A parameter interval $[t_a, t_b]$ corresponds to each such boundary unit of length Δ_g, and these parameter intervals will, in general, not be of the same length despite the fact that all boundary units have equal size.

Importantly, each such boundary unit will have one contact point associated with it, which remains a valid assumption as long as the length of the boundary unit is smaller than the distance between any two boundary points of S that are in contact with the boundary of the set swept by S at *any* parameter t of M.

Traversing the computed sweep boundary points – one boundary unit at a time, collecting all parametric intervals $[t_a, t_b]$, and aligning them on the real line results in a finer discretization of the parametric interval $[0, 1]$ because some of these intervals overlap. By adding the corresponding contact points within each such parametric interval, we obtain the number of contact points for each interval as shown in Figure 3(b). Clearly, the smaller the size of the boundary unit the higher the accuracy of predicting contact changes, which is limited by the resolution of the original sampling. It is important to note that computing the number of contact points based on the Manhattan distance metric results in the correct number of contact points

distance between the centers of two adjacent partial cells varies during the motion: it is minimum when the angle between the tangent and the x axis is a multiple of $\pi/2$, and maximum when the angle is a multiple of 45^o. Note that similar effects can be observed for any alignment of the octree cells.

and correct values of the motion parameter where contact changes occur up to the resolution prescribed by Δ_g.

Let's re-examine the case shown in Figure 1. The computed number of contact points between this moving circular follower and its boundary has been computed based on Manhattan distance metric as described above and illustrated in Figure 4. This number of contact points is two everywhere in Figure 4(a), but is either two or one for the case shown in Figure 4(b). The change in the state of contact occurs at $t = t_{2c}$ and $t = t_{4c}$ where the number of contact points goes down to one and then back to two as t goes from 0 to 1. Here t_{2c} and is t_{4c} are the computed values of the parameter t where contact changes are expected to occur. Note that the computed state of contact is the same as the estimated one shown in Figures 1(c) and (d).

3 Examples

In this section we describe three examples to verify our prototype implementation and illustrate some of the main capabilities of our approach to detect contact changes between a moving object and the boundary of its swept set. We used our sweep boundary evaluator described in [23] implemented in Visual Studio and Parasolid.

The first example in Figure 5 shows a planar non-convex shape moving according to a planar rigid body motion. Figure 5(a) illustrates the computed boundary of swept set S which translates according to trajectory T. Two intermediate configurations of set S, denoted by S^q and S^p, are also displayed in the same figure. The computed state of contact and the contact changes between S and its boundary envelopes are shown in Figure 5(b).

Our second example in Figure 6(a) shows a flat-faced cam-follower mechanism that moves according to a prescribed motion. For this particular case, the contact between the follower and its boundary envelopes is changing a number of times during a complete cycle of the motion. Our algorithm outputs not only when these changes occur during the motion (i.,e., the corresponding parameter values), but also the state of contact at any parameter value t in terms of the number of contact points between S and the boundary envelopes, as illustrated in Figure 6(b).

The last example focuses on a rotary lobe pump whose lobes rotate around fixed axes in space. Figure 7 illustrates a subset of the relative motion between the two lobes as one of the lobes translates and rotates relative to the second lobe. The computed sweep boundary and several intermediate configurations of the moving lobe are displayed in Figure 7(a).

The computed state of contact shown in Figure 7(b) reveals where and when contact changes occur during the motion. At configuration S^q, the number of contact points is two, while at configuration S^r there is only one contact point. On the other hand, the number of contact points significantly increases at configuration S^p, where the lobe shares with its envelopes a whole curve segment[3].

4 Conclusions

Numerous engineering problems involving moving physical artifacts can be abstracted by a moving solid and its swept set of points. One of these important problems is the design and manufacturing of higher pairs, where the state of contact within the pair dictates the functional behavior of the corresponding mechanism.

In this paper we introduce a new generic approach to perform automatic contact analysis between a moving object and its envelopes that form the boundary of the set swept by the moving shape. Our approach exploits the same space sampling used to perform the sweep boundary evaluation to determine the number of contact points between the object and its boundary envelopes throughout the parameter range defining the motion. Even though we have focused here on the planar case, our approach can be extended to 3-dimensional moving solids by using the Manhattan distance metric to measure the surface area of the boundary units. These boundary units will be 2-dimensional surface patches in a 3D space instead of 1-dimensional curve segments in a 2D space as was the case in this paper. Furthermore, each such boundary unit will have the same area as measured with the Manhattan distance metric proposed in this paper.

The accuracy of the computed state of contact is limited by the quality of the space sampling. This implies that this approach may not detect a change in the state of contact that occurs within a parameter range that is comparable to the parametric resolution dictated by the sampling. For the example illustrated in Figure 3(b), if $t_1 - t_4$ is of the same order of magnitude as $min(t_b - t_a)$ for all partial cells, the changes in contact at t_4 and t_1 could be missed.

It is important to note that our approach is generic in the sense that it can be applied to arbitrarily complex shapes moving according to affine motions (not necessarily rigid). To the best of our knowledge, this is the

[3]In order to be able to show the detail of how the contact changes, Figure 7(b) only shows contact points up to 3.

first approach that is capable of predicting contact changes for shapes of arbitrary complexity. At the same time, this approach can be implemented in any representation scheme that supports curve-solid intersections (for details see [23]), and automates the task of contact analysis between a moving object and its boundary envelopes. Equally important, these contact changes can be detected with practically negligible additional computational cost compared to that of the sweep boundary evaluation itself for solids of arbitrary complexity moving according to general affine motions.

Acknowledgments

This work was supported in part by the National Science Foundation grants CMMI-0555937, CAREER award CMMI-0644769, and CMMI-0733107. All geometric models have been constructed by using Parasolid, courtesy of Siemens PLM Software.

References

[1] Reuleaux, F., 1876. *The Kinematics of Machinery.* Macmillan and Company.

[2] Artobolevsky, I. I., 1975. *Mechanisms in Modern Engineering Design.* MIR publishers, Moscow.

[3] Blackmore, D., Leu, M., and Wang, L., 1997. "The sweep-envelope differential equation algorithm and its application to nc machining verification". *Computer Aided Design,* **29**, pp. 629–637.

[4] Malek, K., Yang, J., Blackmore, D., and Joy, K., 2006. "Swept volumes: Foundations, perspectives, and applications". *International Journal of Shape Modeling,* **12**(1), pp. 87–127.

[5] Ilieş, H., and Shapiro, V., 1999. "The dual of sweep". *Computer Aided Design,* **31**(3), Mar., pp. 185–201.

[6] Erdim, H., and Ilieş, H., 2007. "Detecting and quantifying envelope singularities in the plane". *Computer-Aided Design,* **39**(10), pp. 829–840.

[7] Ilieş, H. T., 2000. "On shaping moving mechanical parts". PhD thesis, University of Wisconsin, Madison.

[8] Yan, H., and Cheng, W., 1999. "Curvature analysis of roller-follower cam mechanisms". *Mathematical and Computer Modelling,* **29**, pp. 69–87.

[9] Yang, S.-C., 2001. "Determination of spherical cam profiles by envelope theory". *Journal of Materials Processing Technology,* **116**(2–3), pp. 128–136.

[10] Tsay, D. M., and Wei, H. M., 1996. "A general approach to the determination of planar and spatial cam profiles". *Journal of Mechanical Design,* **118**, June, pp. 259 – 265.

[11] Litvin, F. L., 1994. *Gear Geometry and Applied Theory.* Prentice-Hall.

[12] Litvin, F., 1997. Development of gear technology and theory of gearing. Tech. Rep. NASA RP1406/ARLTR1500, NASA.

[13] Mimmi, G., and Pennacchi, P., 2000. "Non-undercutting conditions in internal gears". *Mechanism and Machine Theory,* **35**(4), pp. 477–490.

[14] Tseng, R., and Tsay, C., 2001. "Mathematical model and undercutting of cylindrical gears with curvilinear shaped teeth". *Mechanism and Machine Theory,* **36**(11–12), pp. 1189–1202.

[15] Bair, B., 2004. "Computer aided design of elliptical gears with circular-arc teeth". *Mechanism and Machine Theory,* **39**(2), pp. 153–168.

[16] Fong, Z., Chiang, T., and Tsay, C., 2002. "Mathematical model for parametric tooth profile of spur gear using line of action". *Mathematical and Computer Modelling,* **36**(4–5), pp. 603–614.

[17] Argyris, J., Litvin, F., Lian, Q., and Lagutin, S., 1999. "Determination of envelope to family of planar parametric curves and envelope singularities". *Computer Methods in Applied Mechanics and Engineering,* **175**(1–2), pp. 175–187.

[18] Chang, S., Tsay, C., and Wu, L., 1996. "Mathematical model and undercutting analysis of elliptical gears generated by rack cutters". *Mechanism and Machine Theory,* **31**(7), pp. 879–890.

[19] Caine, M., 1993. "The design of shape from motion constraints". PhD thesis, Massachusetts Institute of Technology.

[20] Joskowicz, L., and Sacks, E., 1999. "Computer-aided mechanical design using configuration spaces". *IEEE, Computers in Science and Engineering,* **1**(6), pp. 14–21.

[21] Erdim, H., and Ilieş, H., 2008. Classifying points for sweeping solids. Tech. rep., Computational Design Lab, University of Connecticut, February.

[22] Erdim, H., and Ilieş, H., 2007. "A point membership classification for sweeping solids". In ASME IDETC 2007, Design Automation Conference.

[23] Erdim, H., and Ilieş, H., 2008. "Octree-based boundary evaluation for general sweeps". In TMCE 2008, I. Horváth and Z. Rusák, eds.

[24] Ilies, H., 2006. Continuous collision and interference detection for 3d geometric models. Tech. rep., University of Connecticut, December. under review.

[25] Lorensen, W. E., and Cline, H. E., 1987. "Marching cubes: A high resolution 3D surface construction algorithm". *SIGGRAPH Comput. Graph.,* **21**(4), pp. 163–169.

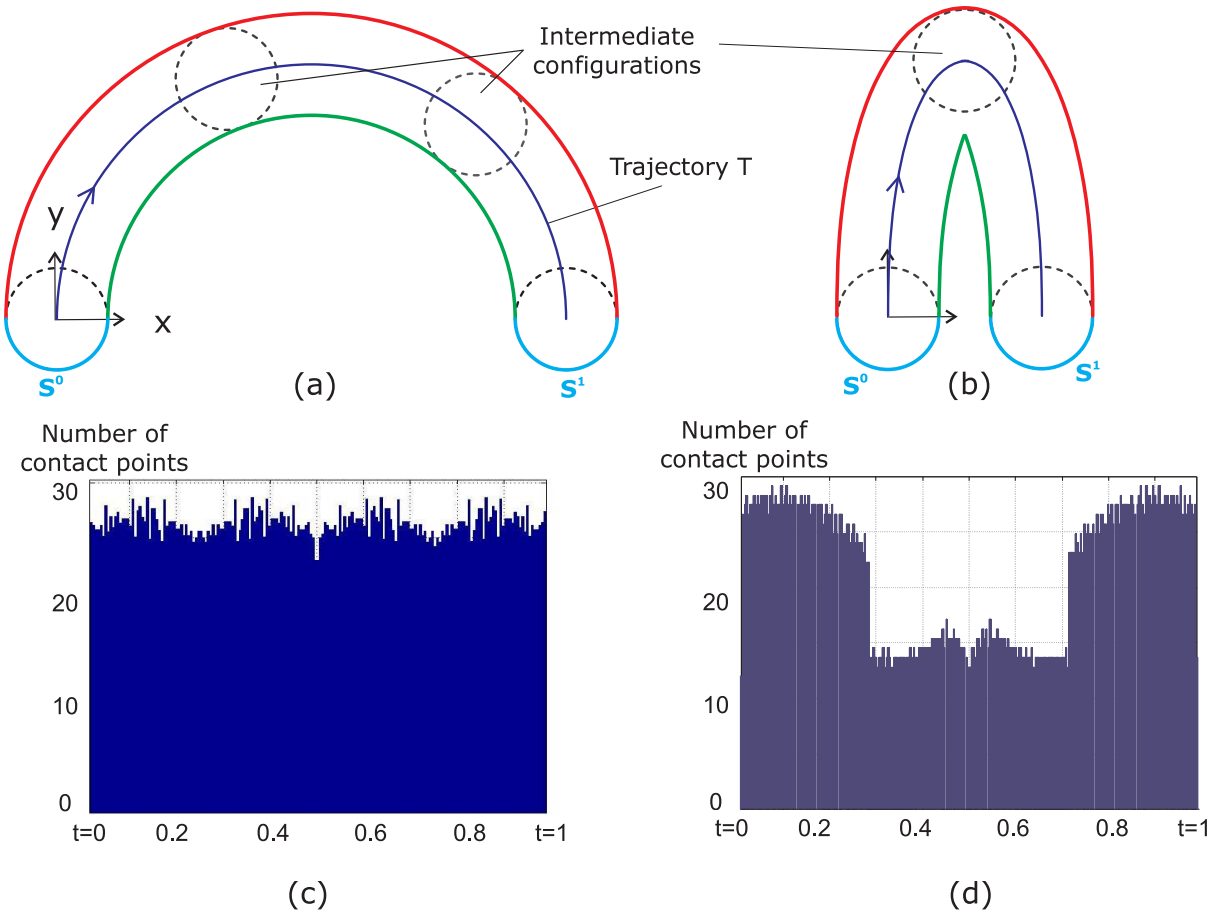

Figure 2: A planar disk S moving according to a circular (a) or elliptical (b) rigid body motion; number of contacts computed based on parametric discretization into 256 equal intervals for the circular motion (c) and the elliptical motion (d).

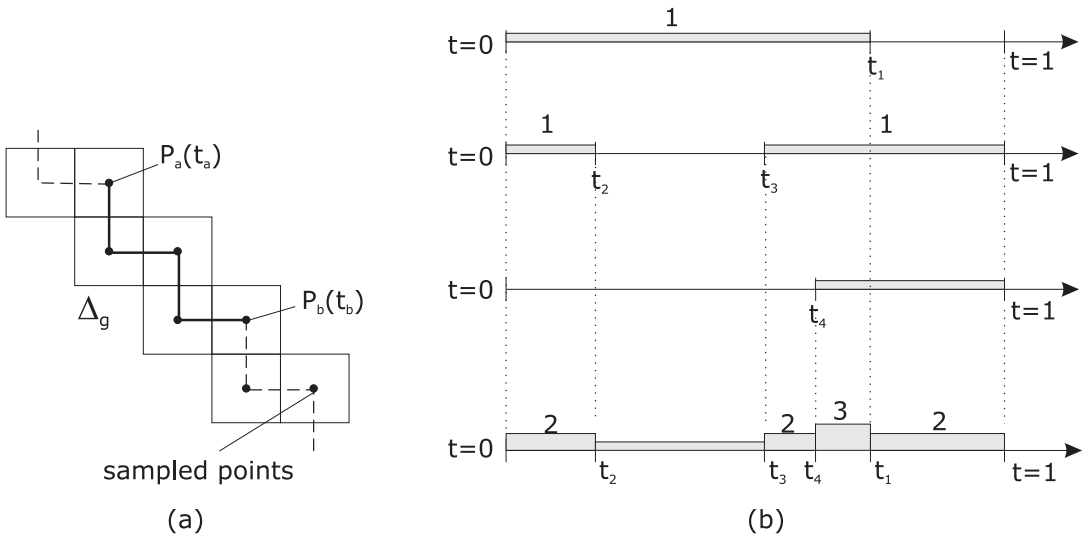

Figure 3: (a) A "Manhattan" distance metric is used to measure boundary units of equal size for our octree-based sampling; (b) estimating the number of contact points between the moving object and its envelopes is achieved by combining the number of contact points for each parameter interval obtained from individual intervals $[t_a, t_b]$. Figure (b) illustrates such a final decomposition of interval $[0, 1]$, and of the final number of contact points.

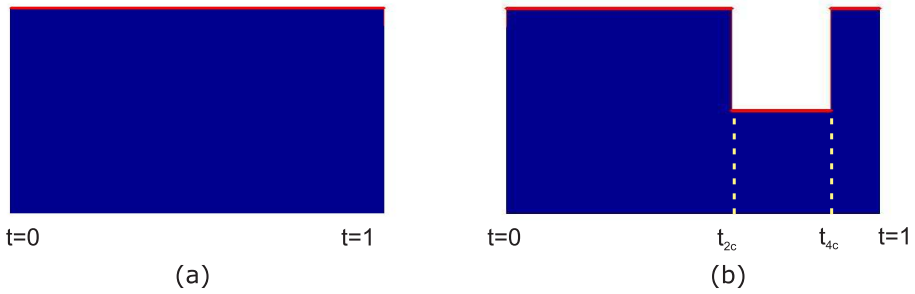

Figure 4: (a) and (b) the computed number of contact points based on Manhattan distance and the octree decomposition of space for the case shown in Figures 1(a) and (b).

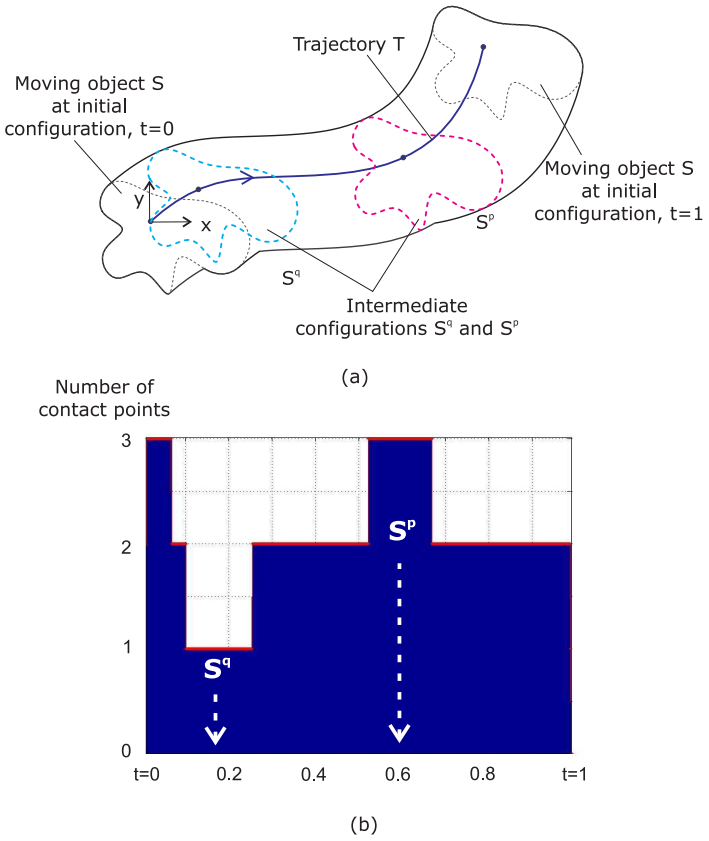

Figure 5: (a) The boundary envelopes of a planar non-convex shape S translating in the plane; (b) the computed state of contact between S and its boundary envelopes.

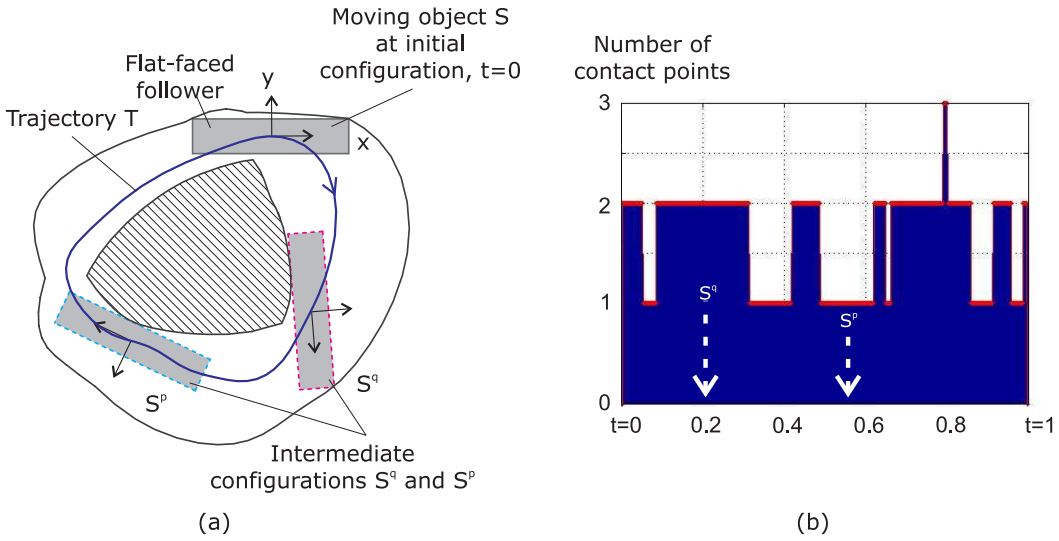

Figure 6: (a) The boundary envelopes of a flat faced cam-follower mechanism moving according to a planar rigid body motion including translation and rotation; (b) the computed state of contact between the follower and its boundary envelopes.

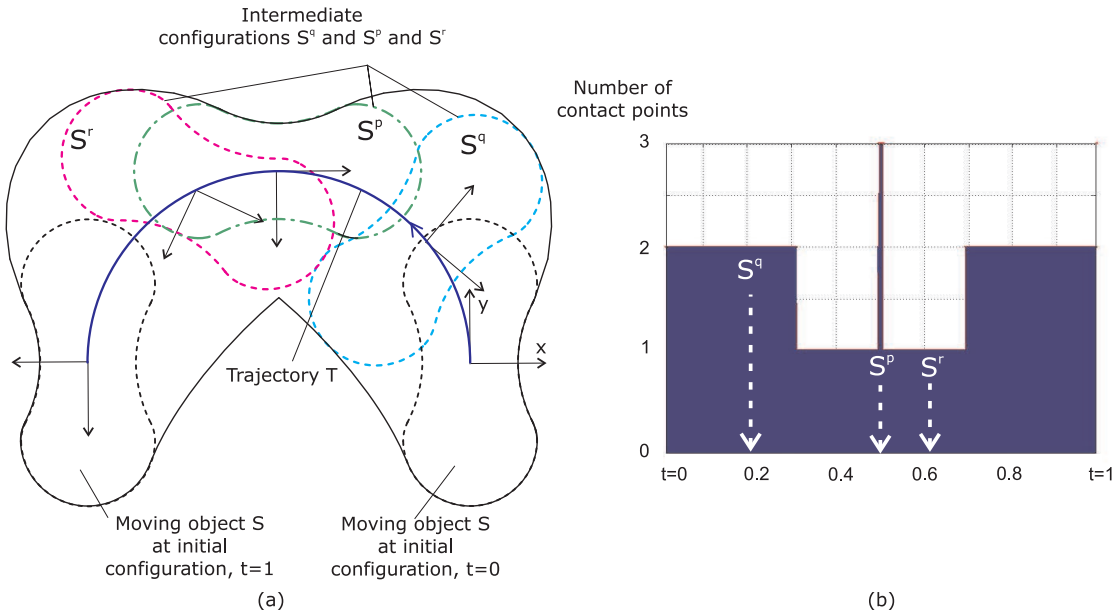

Figure 7: (a) A lobe of a rotary lobe pump moving according to a planar rigid body motion comprised of both translation and rotation; (b) the computed state of contact.